Ferro- and Antiferromagnetic Coupling through 1,*n*-Dithiosquarate Bridges ($n = 2, 3$) in Copper(II) Dimers. Syntheses, Crystal Structures, and Magnetic Properties of $[Cu_2(bpca)_2(1,2\text{-dtsq})(H_2O)]\cdot 2H_2O$ and $[Cu_2(bpca)_2(1,3\text{-dtsq})]\cdot 2H_2O$

Isabel Castro,[1a] María Luisa Calatayud,[1a] Jorunn Sletten,*[,1b] Francesc Lloret,[1a] Juan Cano,[1a] Miguel Julve,*[,1a] Gunther Seitz,[1c] and Klaus Mann[1c]

Departament de Química Inorgànica, Facultat de Química, Universitat de València, Dr. Moliner 50, 46100 Burjassot, València, Spain, Kjemisk Institutt, Universitetet i Bergen, 5007 Bergen, Norway, and Abteilung Pharmazeutische Chemie, Philipps-Universität Marburg, Marbacher Weg 6, 35032 Marburg, Germany

Received April 23, 1999

The preparation, crystal structures, and variable-temperature magnetic susceptibility data for two dithiosquarate-bridged copper(II) complexes of formulas $[Cu_2(bpca)_2(1,2\text{-dtsq})(H_2O)]\cdot 2H_2O$ (**1**) and $[Cu_2(bpca)_2(1,3\text{-dtsq})]\cdot 2H_2O$ (**2**) (where bpca = the bis(2-pyridylcarbonyl)amide anion, 1,2-dtsq = dianion of 3,4-dimercapto-3-cyclobutene-1,2-dione, and 1,3-dtsq = dianion of 3-hydroxy-4-mercapto-2-thioxo-3-cyclobuten-1-one) are reported herein. **1** and **2** crystallize in the triclinic system, space group $P\bar{1}$, with $a = 9.3243(4)$ Å, $b = 10.9036(5)$ Å, $c = 15.5432(4)$ Å, $\alpha = 90.276(2)°$, $\beta = 100.009(2)°$, $\gamma = 94.139(2)°$, and $Z = 2$ for **1** and $a = 7.656(2)$ Å, $b = 9.351(3)$ Å, $c = 11.587(2)$ Å, $\alpha = 109.02(2)°$, $\beta = 97.40(2)°$, $\gamma = 110.27(2)°$, and $Z = 1$ for **2**. Their structures consist of the neutral dithiosquarate-bridged copper(II) units $[Cu_2(bpca)_2(1,2\text{-dtsq})(H_2O)]$ (**1**) and $[Cu_2(bpca)_2(1,3\text{-dtsq})]$ (**2**) and water molecules of crystallization. The copper environment is distorted square pyramidal CuN_3SO in both compounds. Bpca acts as a tridentate end-cap ligand with its three nitrogen atoms occupying three of the four basal positions. 1,3-Dithiosquarate adopts a centrosymmetric bis-bidentate bridging mode with the sulfur atom filling the fourth equatorial position around each copper atom and the oxygen at the apical site. 1,2-Dithiosquarate acts also as a bridging ligand but in an asymmetrical manner, chelating through the two sulfur atoms at one copper atom and unidentate through one sulfur at the other copper atom. The bridging sulfur occupies one equatorial position at a copper atom and the apical site at the other one. The metal−metal separations through the extended 1,2- and 1,3-dtsq bridges are 5.1654(8) and 7.212(3) Å, respectively. The exchange pathways accounting for the intermediate ferro- (**1**, $J = +32.4$ cm^{-1}) and antiferromagnetic (**2**, $J = -33.5$ cm^{-1}) couplings ($\hat{H} = -J\hat{S}_A\cdot\hat{S}_B$) observed in these dithiosquarate-bridged compounds are analyzed and discussed in the light of density functional theory (DFT) calculations.

Introduction

Sulfur-substituted analogues of squarate (dianion of 3,4-dihydroxycyclobut-3-ene-1,2-dione) of formula $C_4O_{4-x}S_x^{2-}$ ($x = 1-4$) are very interesting because of their potential use as chelating (S,S′ or S,O) and/or bis-chelating ligands. Several reports on preparative routes, electronic properties, and reactivity of this family of so-called pseudooxocarbons are available.[2−5] These studies have shown that the exploration of their coordination chemistry is not an easy task because of the hydrolytic and redox reactions they undergo. For the higher sulfur-substituted derivative, namely the tetrathiosquarate dianion ($ttsq^{2-}$), the crystal structure as a potassium salt[6] shows the occurrence of a planar C_4S_4 skeleton with a symmetrical electronic delocalization, the bond orders of C−C and C−S being 1.25 and 1.5, respectively. Structural knowledge of a few of its metal complexes shows that it can adopt bidentate[7] and bis-bidentate[8,9] coordination modes. When $x = 2$, the relative positions of the two sulfur atoms lead to two isomers, which are the 1,2- and 1,3-dithiosquarate dianions (hereafter noted 1,2-dtsq and 1,3-dtsq, respectively). The crystal structures of the 1,2-dtsq-containing metal complexes reveal the preference of this ligand to act as a bidentate ligand through its adjacent sulfur atoms.[5,10−15] This situation contrasts with that of the 1,3-dtsq ligand, where monodentate coordination through sulfur in the mononuclear complex $[Ni(tren)(1,3\text{-dtsq})(H_2O)]$ and bis-biden-

* To whom correspondence should be addressed.

(1) (a) Universitat de València. (b) Universitetet i Bergen. (c) Phillips-Universität Marburg.
(2) (a) Seitz, G.; Imming, P. *Chem. Rev.* **1992**, *92*, 1227. (b) Seitz, G. *Phosphorus, Sulfur Silica* **1989**, *43*, 311.
(3) Carré, B.; Paris, J.; Fabre, P. L.; Jourdannaud, S.; Castan, P.; Deguenon, D.; Wimmer, S. *Bull. Soc. Chim. Fr.* **1990**, *127*, 367.
(4) Eggerding, D.; West, R. *J. Org. Chem.* **1976**, *41*, 3904.
(5) Coucouvanis, D.; Hollander, F. J.; West, R.; Eggerding, D. *J. Am. Chem. Soc.* **1974**, *96*, 3006.
(6) Allmann, R.; Debaerdemaeker, T.; Mann, K.; Matusch, R.; Schmiedel, R.; Seitz, G. *Chem. Ber.* **1976**, *109*, 2208.
(7) Grenz, R.; Götzfried, F.; Nagel, U.; Beck, W. *Chem. Ber.* **1986**, *119*, 1217.
(8) Jones, P. G.; Sheldrick, G. M.; Fügner, A.; Götzfried, F.; Beck, W. *Chem. Ber.* **1981**, *114*, 1413.
(9) Vogt, T.; Faulmann, C.; Soules, R.; Lecante, P.; Mosset, A.; Castan, P.; Cassoux, P.; Galy, J. *J. Am. Chem. Soc.* **1988**, *110*, 1833.
(10) Coucouvanis, D.; Holah, D. G.; Hollander, F. J. *Inorg. Chem.* **1975**, *14*, 2657.
(11) (a) Coucouvanis, D.; Swenson, D.; Baenziger, N. C.; Holah, D. G.; Kostikas, A.; Simopoulos, A.; Petrouleas, V. *J. Am. Chem. Soc.* **1976**, *98*, 5721. (b) Coucouvanis, D.; Swenson, D.; Baenziger, N. C.; Murphy, C.; Holah, D. G.; Sfarnas, N.; Simopoulos, A.; Kostikas, A. *J. Am. Chem. Soc.* **1981**, *103*, 3350.
(12) Altmeppen, D.; Mattes, R. *Acta Crystallogr., Sect. B* **1980**, *36*, 1942.

10.1021/ic9904384 CCC: $18.00
Published on Web 10/01/1999

tate coordination through the sulfur−oxygen pair in the dinuclear complex $[Ni_2(tren)_2(1,3\text{-dtsq})](ClO_4)_2$ were observed by us recently.[16]

In the present work, we report the synthesis, structural characterization, and magnetic study of the first 1,2- and 1,3-dtsq-bridged copper(II) dinuclear compounds of formulas $[Cu_2(bpca)_2(1,2\text{-dtsq})(H_2O)]\cdot 2H_2O$ (**1**) and $[Cu_2(bpca)_2(1,3\text{-dtsq})]\cdot 2H_2O$ (**2**), where bpca is the bis(2-pyridylcarbonyl)amide anion. Theoretical calculations aiming at analyzing the exchange pathways responsible for the moderate intramolecular ferro- (**1**) and antiferromagnetic (**2**) coupling and the influence of the relative positions of the sulfur atoms of the 1,*n*-dithiosquarate bridge on the magnitude and sign of magnetic interactions are also presented.

Experimental Section

Materials. The starting products, $K_2(1,2\text{-dtsq})\cdot H_2O$, $K_2(1,3\text{-dtsq})\cdot 2H_2O$, and $[Cu(bpca)(H_2O)_2]NO_3\cdot 2H_2O$, were prepared as reported in the literature.[4,17,18] Elemental analyses (C, H, N, S) were performed by the Microanalytical Service, Universidad Autónoma de Madrid.

Preparation of Compounds. $[Cu_2(bpca)_2(1,2\text{-dtsq})(H_2O)]\cdot 2H_2O$ (1). This complex was prepared by adding 0.018 g of $K_2(1,2\text{-dtsq})\cdot H_2O$ ($^1/_{12}$ mmol) dissolved in a minimum amount of water to an aqueous solution (50 mL) containing 0.073 g of $[Cu(bpca)(H_2O)_2]NO_3\cdot 2H_2O$ ($^1/_6$ mmol). The addition of the dithiosquarate caused a color change of the solution from blue to green. Green parallelepipeds of **1** which were suitable for X-ray diffraction grew from the mother liquor by evaporation at 28 °C after a few hours. They were filtered off and washed with cold water, ethanol, and diethyl ether. Anal. Calcd for $C_{28}H_{22}Cu_2N_6O_9S_2$ (**1**): C, 43.20; H, 2.80; N, 10.80; S, 8.20. Found: C, 43.20; H, 2.40, N, 11.00; S, 7.90.

The remaining slightly colored solution is not stable, as evidenced by the small amount of a crystalline green solid of formula $Cu_2(bpca)_2(ox)\cdot 4H_2O$ (ox is the oxalate dianion) that separated on standing after several days. The presence of oxalate is supported by analytical (C, H, N) and infrared data.

$[Cu_2(bpca)_2(1,3\text{-dtsq})]\cdot 2H_2O$ (2). This compound was prepared by adding 0.030 g of $K_2(1,3\text{-dtsq})\cdot 2H_2O$ ($^1/_8$ mmol) dissolved in a minimum amount of water to an aqueous solution (50 mL) of 0.106 g of $[Cu(bpca)(H_2O)_2]NO_3\cdot 2H_2O$ ($^1/_4$ mmol). The initial blue solution turned green with the subsequent formation of a yellow-greenish crystalline solid of **2** in a nearly quantitative yield. This was filterd off and washed with cold water, ethanol, and diethyl ether. All our attempts to obtain single crystals of **2** in aqueous solution were unsuccessful. However, rhombohedral crystals of **2** of X-ray diffraction quality were grown by the gel technique using agarose as gel. In a successful typical experiment, aqueous solutions of $[Cu(bpca)(H_2O)_2]NO_3\cdot 2H_2O$ (0.01 mol dm^{-3}) and $K_2(1,3\text{-dtsq})\cdot 2H_2O$ (0.004 mol dm^{-3}) were diffused through agarose gel (1%). This gel was obtained by heating an agarose suspension at 60 °C during 1 h. Anal. Calcd for $C_{28}H_{20}Cu_2N_6O_8S_2$ (**2**): C, 44.26; H, 2.65; N, 11.06; S, 8.14. Found: C, 44.20; H, 2.72; N, 11.12; S, 7.94.

Physical Measurements. Infrared spectra were recorded on a Perkin-Elmer 1750 FTIR spectrophotometer on a KBr pellet in the 4000−400 cm^{-1} region, and electronic spectra in dmso solution and as Nujol mull samples were measured on a Perkin-Elmer Lambda 9 spectrophotometer. Magnetic susceptibility measurements of polycrystalline samples were measured over the temperature range 2.0−290 K with a Quantum Design SQUID susceptometer and using an applied magnetic field of 0.1 T. Independence of the magnetic susceptibility as a function of the magnetic field was checked for compound **1**. The susceptometer was calibrated with $(NH_4)_2Mn(SO_4)_2\cdot 12H_2O$. Diamagnetic corrections of the constituent atoms were calculated from Pascal's constants[19] and found to be -389×10^{-6} and -380×10^{-6} cm^3 mol^{-1} for **1** and **2**, respectively. The value of 60×10^{-6} cm^3 mol^{-1} was used for the temperature-independent paramagnetism of the copper(II) ion.

Computational Methodology. The computational strategy used in the present work has been fully described elsewhere,[20] and it is briefly outlined here. Density functional theory[21] was used to evaluate the coupling constants of **1** and **2**. Two separate calculations were done, one for the triplet and another for a broken-symmetry singlet state. The hybrid B3LYP method[22] was been used in the calculations as implemented in Gaussian 94,[23] mixing the exact Hartree−Fock exchange with Becke's expression for the exchange[24] and using the Lee−Yang−Parr correlation functional.[25] Basis sets of triple-ζ[26] (copper atoms) and of double-ζ quality[27] (atoms other than copper) were used in all calculations.

The singlet−triplet energy gap (J) was evaluated from the calculated energies of the triplet (E_{HS}) and broken-symmetry singlet (E_{BS}) spin states through eq 1,

$$J = \frac{2(E_{BS} - E_{HS})}{S(S+1)} \tag{1}$$

where S is the total spin for the high-spin state. Model systems of **1** and **2** where the bpca nitrogen atoms have been replaced by three ammonia groups (but the bond lengths and angles are those of the real structures) were used to analyze the exchange pathways in these compounds. Once this was done, the complete dimeric structures (bpca ligands included) were used in the calculations to estimate the values of J.

Crystallographic Data Collection and Structure Determination. Compound 1. Diffraction data of **1** were collected at 223 K on a crystal of dimensions $0.28 \times 0.19 \times 0.08$ mm with a 2K SMART CCD area detector diffractometer using ω rotation scans, a scan width of 0.3°, and graphite-monochromated Mo Kα radiation ($\lambda = 0.710\,73$ Å). Crystal parameters and refinement results are listed in Table 1. A total of 24 800 reflections were measured within 2θ of 56.7°; 7737 reflections were independent. Due to modest crystal quality, the diffraction profiles were quite irregular; this accounts for the high internal agreement factor between symmetry-related reflections ($R_{int} = 0.1067$). Absorption corrections were done by numerical integration.

The structure was solved by direct methods and refined by full-matrix least-squares refinement, based on F^2 and including all reflections. One of the uncoordinated water molecules is disordered; two fractional oxygen sites were refined, the occupancy factors converging at 0.30 and 0.70, respectively. All non-hydrogen atoms were anisotropically refined. Hydrogen atoms attached to carbons were included at

(13) (a) Arrizabalaga, Ph.; Bernardinelli, G.; Castan, P.; Geoffroy, M.; Soules, R. *C. R. Acad. Sci., Ser. 2* **1987**, *304*, 559. (b) Krause, R.; Mattes, R. *Z. Naturforsch., Chem. Sci.* **1990**, *45B*, 490.
(14) (a) Bonnet, J. J.; Cassoux, P.; Castan, P.; Laurent, J. P.; Soules, R. *Mol. Cryst. Liq. Cryst.* **1987**, 142, 113. (b) Arrizabalaga, Ph.; Bernardinelli, G.; Geoffroy, M. *Inorg. Chim. Acta* **1988**, *154*, 35.
(15) Engel, G.; Mattern, G. *Z. Anorg. Allg. Chem.* **1994**, *620*, 723.
(16) Calatayud, M. L.; Castro, I.; Sletten, J.; Cano, J.; Lloret, F.; Faus, J.; Julve, M.; Seitz, G.; Mann, K. *Inorg. Chem.* **1996**, *35*, 2858.
(17) (a) Seitz, G.; Mann, K.; Schmiedel, R.; Matusch, R. *Chem. Ber.* **1979**, *112*, 990, (b) Mattes, R.; Johann, G. *Acta Crystallogr., Sect. C* **1984**, *40*, 740.
(18) Castro, I.; Faus, J.; Julve, M.; Amigó, J. M.; Sletten, J.; Debaerdemaeker, T. *J. Chem. Soc., Dalton Trans.* **1990**, 891.
(19) Earshaw, A. *Introduction to Magnetochemistry*; Academic Press: London and New York, 1968.
(20) Ruiz, E.; Alemany, P.; Alvarez, S.; Cano, J. *J. Am. Chem. Soc.* **1997**, *119*, 1297.
(21) Parr, R. G.; Yang, W. *Density Functional Theory of Atoms and Molecules*; Oxford University Press: New York, 1989.
(22) Becke, A. D. *J. Chem. Phys.* **1993**, *98*, 5648.
(23) Frisch, M. J.; Trucks, G. W.; Schlegel, H. B.; Gill, P. M. W.; Johnson, B. G.; Robb, M. A.; Cheeseman, J. R.; Keith, T. A.; Petersson, G. A.; Montgomery, J. A.; Raghavachari, K.; Al-Laham, M. A.; Zakrzewski, V. G.; Ortiz, J. V.; Foresman, J. B.; Cioslowski, J.; Stefanov, B.; Nanayakkara, A.; Challacombe, M.; Peng, C. Y.; Ayala, P. Y.; Chen, W.; Wong, M. W.; Andres, J. L.; Replogle, E. S.; Gomperts, R.; Martin, R. L.; Fox, D. J.; Binkley, J. S.; Defrees, D. J.; Baker, J. P.; Stewart, J. P.; Head-Gordon, M.; González, C.; Pople, J. A. *Gaussian 94*, Revision C.3; Gaussian Inc.: Pittsburgh, PA, 1995.
(24) Becke, A. D. *Phys. Rev. A* **1988**, *38*, 3098.
(25) Lee, C.; Yang, W.; Parr, R. G. *Phys. Rev. B* **1988**, *37*, 785.
(26) Schaefer, A.; Huber, C.; Ahlrichs, R. *J. Chem. Phys.* **1994**, *100*, 5829.
(27) Schaefer, A.; Horn, H.; Ahlrichs, R. *J. Chem. Phys.* **1992**, *97*, 2571.

Table 1. Summary of Crystallographic Data and Structure Refinement for $[Cu_2(bpca)_2(1,2\text{-dtsq})(H_2O)]\cdot 2H_2O$ (**1**) and $[Cu_2(bpca)_2(1,3\text{-dtsq})]\cdot 2H_2O$ (**2**)

	1	**2**
empirical formula	$Cu_2C_{28}H_{22}N_6O_9S_2$	$Cu_2C_{28}H_{20}N_6O_8S_2$
fw	777.72	759.70
space group	$P\bar{1}$	$P\bar{1}$
a/Å	9.3243(4)	7.656(2)
b/Å	10.9036(5)	9.351(3)
c/Å	15.5432(4)	11.587(2)
α/deg	90.276(2)	109.02(2)
β/deg	100.009(2)	97.40(2)
γ/deg	94.139(2)	110.27(2)
V/Å^3	1551.90(11)	707.8(3)
Z	2	1
ρ(calcd)/(g cm^{-3})	1.664	1.782
λ/Å	0.710 73	0.710 73
T/K	223(2)	294(2)
μ/cm^{-1}	15.68	17.15
R^a	0.0662	0.0900
$R_w{}^{b,c}$	0.1612	0.2133

[a] $R = \sum||F_o| - |F_c||/\sum|F_o|$. [b] $R_w = \{\sum[w(F_o^2 - F_c^2)^2]/\sum[w(F_o^2)^2]\}^{1/2}$. [c] $w = 1/\sigma^2(F_o^2) + (AP)^2 + BP$, where $P = [(\text{maximum of } 0 \text{ or } F_o^2) + 2F_c^2]/3$, $A = 0.0820$ (**1**) and 0.1636 (**2**), and $B = 2.96$ (**1**) and 0.00 (**2**).

idealized positions; hydrogen atoms of water molecules could not be located in difference Fourier maps and were not included in the structure factor calculations. The refinement converged at a conventional R factor of 0.0662 (for 5033 reflections with $I > 2\sigma_I$). The final difference Fourier map showed residual densities between +1.23 and −1.17 e Å^{-3}. The goodness of fit on F^2 was 1.014, and the data/restraint/parameter ratio was 7737/0/433. For data collection and data integration, the SMART and SAINT programs were used;[28] all other calculations were done with the SHELXTL program system.[29,30] Main bond distances and angles are listed in Table 2.

Compound 2. Diffraction data of **2** were collected at 293 K on a crystal of dimensions 0.57 × 0.09 × 0.026 mm with an Enraf-Nonius CAD-4 diffractometer, using graphite-monochromated Mo Kα radiation (λ = 0.710 73 Å). The data collection was conducted at room temperature, as the thin and fragile crystals tended to crack when being cooled. Crystal parameters and refinement results are listed in Table 1. Cell dimensions were determined on the basis of setting angles of 25 reflections in the 2θ range 30−38°. A total of 2752 reflections within 2θ = 50.0° were recorded using the $\omega/2\theta$ scan technique. Three reference reflections monitored throughout the data collection showed a gradual decay amounting in average to 8%. The data were corrected for absorption on the basis of ψ-scan measurements using six reflections.[31] Several crystals were screened before data collection; all displayed split reflections. After inspection of the intensity data, 17 reflections with large negative values of the net intensities or unreasonably uneven background counts were suppressed in the calculations.

The structure was solved by the Patterson method and completed by subsequent Fourier maps. In the course of the full-matrix least-squares refinement, based on F^2 and including all reflections, it became clear that the noncoordinated water molecule was disordered. Two fractional oxygen positions were isotropically refined, and occupancy factors of the two sites converged at 0.55 and 0.45, respectively. The remaining non-hydrogen atoms were anisotropically refined. Hydrogen atoms bound to carbon were included in the model at idealized positions. Hydrogen atoms of water molecules could not be located in difference Fourier maps and were not included in the structure factor calculations. The refinement converged at a conventional R factor of 0.0900 (for 1684 reflections with $I > 2\sigma_I$). The final difference Fourier map showed residual densities between +1.99 and −1.55 e Å^{-3}. The goodness of fit on F^2 is 1.084, and the data/restraint/parameter ratio was 2381/0/207. Due to the occurrence of disorder, the structure was also solved and refined in space group $P1$. The refinement gave, however, unreasonable distances and high correlation coefficients. Data reduction was done with the XCAD program.[32] All other calculations were performed with the SHELXS-86, SHELXL-93, and XPL programs.[30,33] Main bond distances and angles are listed in Table 3.

Table 2. Main Bond Lengths (Å) and Angles (deg) for $[Cu_2(bpca)_2(1,2\text{-dtsq})(H_2O)]\cdot 2H_2O$ (**1**)[a]

	Copper Coordination Sphere		
Cu(1)−N(2)	1.929(5)	Cu(2)−N(5)	1.956(4)
Cu(1)−N(3)	2.000(6)	Cu(2)−N(6)	2.024(4)
Cu(1)−N(1)	2.071(6)	Cu(2)−N(4)	2.027(4)
Cu(1)−S(2)	2.2804(13)	Cu(2)−S(1)	2.3240(12)
Cu(1)−S(1)	2.9137(12)	Cu(2)−O(7)	2.359(4)
N(2)−Cu(1)−N(3)	84.0(3)	N(5)−Cu(2)−N(6)	80.68(16)
N(2)−Cu(1)−N(1)	81.1(3)	N(5)−Cu(2)−N(4)	81.41(17)
N(3)−Cu(1)−N(1)	164.7(2)	N(6)−Cu(2)−N(4)	160.59(16)
N(2)−Cu(1)−S(2)	173.63(15)	N(5)−Cu(2)−S(1)	176.63(12)
N(3)−Cu(1)−S(2)	98.29(15)	N(6)−Cu(2)−S(1)	98.85(11)
N(1)−Cu(1)−S(2)	96.09(16)	N(4)−Cu(2)−S(1)	98.59(12)
N(2)−Cu(1)−S(1)	95.97(15)	N(5)−Cu(2)−O(7)	98.01(15)
N(3)−Cu(1)−S(1)	95.02(12)	N(6)−Cu(2)−O(7)	96.70(16)
N(1)−Cu(1)−S(1)	90.33(12)	N(4)−Cu(2)−O(7)	93.14(16)
S(2)−Cu(1)−S(1)	89.76(4)	S(1)−Cu(2)−O(7)	85.36(9)
	1,2-dtsq Ligand		
S(1)−C(13)	1.694(5)	C(13)−C(14)	1.390(6)
S(2)−C(14)	1.709(4)	C(13)−C(16)	1.475(7)
O(3)−C(15)	1.201(6)	C(14)−C(15)	1.478(7)
O(4)−C(16)	1.208(6)	C(15)−C(16)	1.547(7)
C(13)−S(1)−Cu(2)	102.53(16)	C(13)−C(14)−S(2)	132.5(4)
C(13)−S(1)−Cu(1)	84.81(15)	C(15)−C(14)−S(2)	134.3(3)
Cu(2)−S(1)−Cu(1)	160.82(6)	O(3)−C(15)−C(14)	135.7(5)
C(14)−S(2)−Cu(1)	98.22(15)	O(3)−C(15)−C(16)	137.6(5)
C(14)−C(13)−C(16)	92.8(4)	C(14)−C(15)−C(16)	86.6(4)
C(14)−C(13)−S(1)	132.7(4)	O(4)−C(16)−C(13)	135.3(5)
C(16)−C(13)−S(1)	134.5(4)	O(4)−C(16)−C(15)	137.4(5)
C(13)−C(14)−C(15)	93.3(4)	C(13)−C(16)−C(15)	87.3(4)

[a] Estimated standard deviations in the least significant digits are given in parentheses.

Results and Discussion

Descriptions of Structures. $[Cu_2(bpca)_2(1,2\text{-dtsq})(H_2O)]\cdot 2H_2O$ (1). The structure of **1** consists of neutral, 1,2-dtsq-bridged copper(II) units of the formula $[Cu_2(bpca)_2(1,2\text{-dtsq})(H_2O)]$ (Figure 1) and waters of crystallization. The two copper ions both have distorted square pyramidal coordination geometries. The equatorial planes are defined by three bpca nitrogen atoms (Cu−N in the ranges 1.930−2.071 Å for Cu(1) and 1.956−2.027 Å for Cu(2)) and one of the dtsq sulfur atoms (Cu(1)−S(2) = 2.280 Å and Cu(2)−S(1) = 2.324 Å), while the apical position is occupied in the case of Cu(1) by a dtsq sulfur atom (Cu(1)−S(1) = 2.914 Å) and in the case of Cu(2) by a water molecule (Cu(2)−O(7) = 2.359 Å). The equatorial planes display slight tetrahedral distortions, the copper atoms being displaced by 0.094 Å (Cu(1)) and 0.101 Å (Cu(2)) from the planes toward the respective apical ligands. The dihedral angle between the equatorial planes of the two copper atoms is 86.5°. Two centrosymmetrically related dinuclear units are loosely connected into tetranuclear entities by weak Cu···S interactions

(28) *SMART, Data Collection Software,* Version 4.0, and *SAINT, Data Integration Software,* Version 4.0; Bruker AXS, Inc.: Madison, WI, 1997.
(29) Sheldrick, G. M. *Acta Crystallogr., Sect. A* **1990**, *46*, 467.
(30) *SHELXTL*, Version 5.1; Bruker AXS, Inc.: Madison, WI, 1997.
(31) (a) North, A. C. T.; Phillips, D. C.; Mathews, F. S. *Acta Crystallogr., Sect. A* **1968**, *24*, 351. (b) Kopfman, G.; Huber, R. *Acta Crystallogr., Sect. A* **1968**, *24*, 348.
(32) Harms, K. *XCAD*; Fachbereich Chemie, Philipps-Universität Marburg: Marburg, Germany.
(33) Sheldrick, G. M. *SHELXL-93*; University of Göttingen: Göttingen, Germany, 1993. Sheldrick, G. M. *SHELXTL-PLUS*, Version 4.21; Siemens Analytical X-ray Instruments, Inc.: Madison, WI, 1990.

Table 3. Main Bond Lengths (Å) and Angles (deg) for $[Cu_2(bpca)_2(1,3\text{-dtsq})]\cdot 2H_2O$ (**2**)[a,b]

Copper Coordination Sphere			
Cu−N(2)	1.963(7)	Cu−S	2.324(3)
Cu−N(1)	2.013(7)	Cu−O(3)	2.590(7)
Cu−N(3)	2.032(8)	Cu−O(1b)	2.903(8)
N(2)−Cu−N(1)	81.5(3)	N(3)−Cu−O(3)	84.1(3)
N(2)−Cu−N(3)	81.6(3)	S−Cu−O(3)	86.2(2)
N(1)−Cu−N(3)	163.0(3)	N(2)−Cu−O(1b)	91.5(3)
N(2)−Cu−S	175.1(2)	N(1)−Cu−O(1b)	94.3(3)
N(1)−Cu−S	99.4(2)	N(3)−Cu−O(1b)	84.5(3)
N(3)−Cu−S	97.3(2)	S−Cu−O(1b)	83.6(2)
N(2)−Cu−O(3)	98.4(3)	O(3)−Cu−O(1b)	163.6(2)
N(1)−Cu−O(3)	100.0(3)		
1,3-dtsq Ligand			
S−C(13)	1.688(9)	C(14)−C(13)−C(14a)	91.2(7)
O(3)−C(14)	1.236(11)	C(14)−C(13)−S	129.7(7)
C(13)−C(14)	1.415(13)	C(14a)−C(13)−S	139.1(7)
C(13)−C(14a)	1.470(11)	O(3)−C(14)−C(13)	133.2(8)
C(13)−S−Cu	92.9(3)	O(3)−C(14)−C(13a)	138.0(9)
C(14)−O(3)−Cu	96.3(6)	C(13)−C(14)−C(13a)	88.8(7)

[a] Estimated standard deviations in the least significant digits are given in parentheses. [b] Symmetry transformations used to generate equivalent atoms: (a) $-x, 1-y, 1-z$; (b) $-x, -y, -z$.

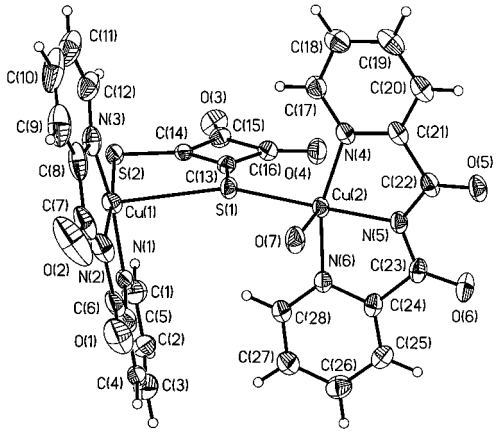

Figure 1. Perspective view of the $[Cu_2(bpca)_2(1,2\text{-dtsq})(H_2O)]$ dinuclear unit of **1**. Thermal ellipsoids are plotted at the 30% probability level.

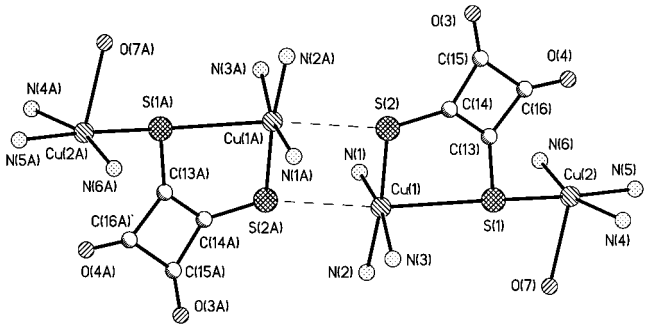

Figure 2. View of the tetranuclear arrangement in **1** (Cu(1)···S(2a) = 3.207(1) Å; symmetry code a = $1-x, 1-y, -z$).

[Cu(1)···S(2a) = 3.207(1) Å; (a) = $1-x, 1-y, -z$], this sulfur atom is thus occupying the second axial position of Cu(1) (Figure 2). The proximity of one of the dtsq oxygen atoms (Cu(2)···O(4) = 3.242(5) Å) screens the second axial position of Cu(2). The equatorial Cu−S distances observed in this compound are comparable with those reported in two previous studies of copper(II)−1,2-dithiosquarate complexes, $[Cu(en)_2][Cu(1,2\text{-dtsq})_2]$ (average Cu−S = 2.302 Å)[13b] and $[P(Ph)_4]_2[Cu(1,2\text{-dtsq})_2]$ (average Cu−S = 2.326 Å).[13a] In the former case, also a Cu···S axial interaction of 3.057 Å is found between a 1,2-dtsq sulfur and the copper of the complex cation.[13b]

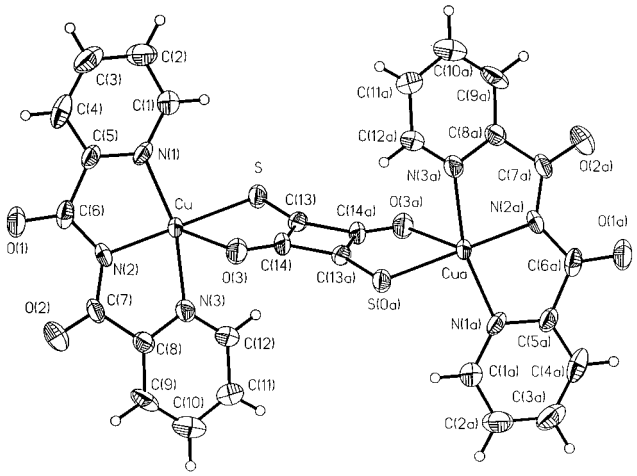

Figure 3. Perspective view of the $[Cu_2(bpca)_2(1,3\text{-dtsq})]$ dinuclear unit in **2**. Thermal ellipsoids are plotted at the 50% probability level.

The 1,2-dtsq group acts as a monodentate ligand toward Cu(2), coordinating through S(1), and as an asymmetric, chelating S,S ligand, coordinating toward Cu(1); S(1) thus forms a monatomic bridge between the two metal centers, the Cu(1)−S(1)−Cu(2) angle being 160.8°. The endo chelate S−C−C angles (132.5° in average) are slightly smaller than the corresponding exo chelate angles (134.4° on average), the S···S bite distance in the complex being 3.692 Å. For the uncomplexed ligand, a bite of 3.75 Å has been estimated by assuming S−C−C angles of 134°.[10] The shortening due to chelate formation with a 3d metal is thus small in the present structure; this is related to the asymmetric chelation and to the bridging function of S(1). The bond lengths of 1,2-dtsq compare well with those observed previously in such metal-coordinated groups.[5,10−15] The 1,2-dtsq group is almost planar, and the Cu atoms deviate by 0.495 Å (Cu(1)) and 0.365 Å (Cu(2)) from this plane. The dihedral angles between the copper equatorial planes and dtsq are 79.1° (Cu(1)) and 85.3° (Cu(2)).

The intramolecular Cu(1)···Cu(2) distance across the 1,2-dtsq bridge is 5.1654(8) Å. The Cu(1)···Cu(1a) distance of 4.285(1) Å is the shortest metal−metal distance observed and occurs across the weak Cu(1)···S(2a)−Cu(1a) interaction within the tetrameric entity described above (see Figure 2). The only other metal−metal distance below 7 Å, Cu(2)···Cu(2b) = 6.707(1) Å (b = $2-x, -y, 1-z$), occurs between units linked through hydrogen bonds between the coordinated water molecule and bpca oxygen atoms [2.990(6) and 2.840(5) Å for O(7)···O(5b) and O(7)···O(6b), respectively]. Although the water hydrogen atoms could not be located, a consistent hydrogen-bonding pattern can be derived on the basis of O···O distances and available hydrogen donors. The two disordered water molecules have different hydrogen bonds, and the major site (occupancy 0.70) participates in four hydrogen bonds, while the minor site (occupancy 0.30) participates in three of them.

$[Cu_2(bpca)_2(1,3\text{-dtsq})]\cdot 2H_2O$ (2). The structure consists of neutral, 1,3-dtsq-bridged dinuclear units, $[Cu_2(bpca)_2(1,3\text{-dtsq})]$ (Figure 3), and waters of hydration. The copper atom has a distorted square pyramidal coordination geometry with the three bpca nitrogen atoms and the 1,3-dtsq sulfur atom in the equatorial plane (Cu−N = 1.963−2.032 Å, Cu−S = 2.324 Å) and a dtsq oxygen atom in the apical position (Cu−O(3) = 2.590 Å). There is a slight tetrahedral distortion of the equatorial plane,

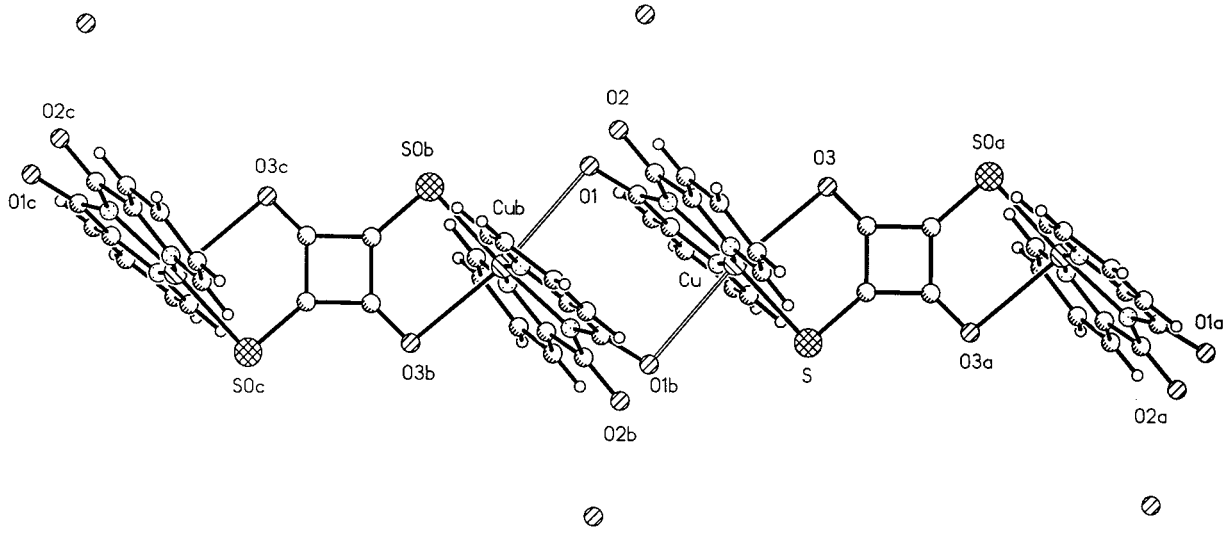

Figure 4. A fragment of the chain structure in **2** showing the weak Cu···O(1) axial interactions. Hydrogen atoms have been omitted for clarity. Symmetry operations: (a) $-x, 1-y, 1-z$; (b) $-x, -y, -z$; (c) $x, -1+x, -1+z$.

and the copper atom is displaced 0.066 Å from this plane toward the apical O(3). Molecules related by centers of symmetry are arranged into chains, running parallel to the *bc* diagonal, such that Cu has a close contact to the bpca oxygen atom O(1) of the neighboring unit, Cu−O(1b) = 2.903 Å (b = $-x, -y, -z$) (Figure 4). O(1b) thus occupies the second axial position on Cu. Despite the fact that this Cu−O distance is on the long side of what is usually considered, even for semicoordination,[34] there is structural evidence of a bonding interaction. O(1) is bent out of the plane of the chelate ring Cu,N(1),C(5),C(6),-N(2) by 0.218 Å in the direction toward Cu(b), while O(2), by comparison, is 0.085 Å out of the plane of the Cu,N(3),C(8),-C(7),N(2) chelate ring in the opposite direction. A corresponding interaction is also present in the $[Cu_2(bpca)_2(C_5O_5)]\cdot 3H_2O$ structure.[35]

The 1,3-dtsq group acts as a bis-bidentate ligand, S coordinating equatorially and O(3) axially to Cu. To accommodate the chelating coordination mode, the endo angles S−C(13)−C(14) and O(3)−C14)−C(13) are narrowed down to 129.7 and 133.2° as compared to the exo angles at the dithiosquarate carbon atoms, S−C(13)−C(14a) of 139.1° and O(3)−C(14)−C(13a) of 138.0°. This allows for a S···O(3) bite distance in the complex of 3.363(7) Å, while the S···O(3a) distance is 3.675(7) Å. This distortion of the 1,3-dtsq group is slightly smaller than the distortion observed in $[Ni_2(tren)_2(1,3\text{-dtsq})](ClO_4)_2$.[16] The 1,3-dtsq group is essentially planar, and the Cu atom deviates by 0.436 Å from the dtsq mean plane. The dihedral angle between the copper equatorial plane and the dtsq plane is 73.7(1)°.

The intradimer Cu···Cu(a) distance across the 1,3-dtsq bridge is 7.212(3) Å. The shortest intermolecular metal−metal separation is Cu···Cu(b) = 5.079(2) Å and occurs between copper atoms bridged by the very weak axial Cu···O(1) interaction in the chain (Figure 4). Although hydrogen atoms of the disordered water molecule could not be located, a survey of intermolecular O···O and O···S distances indicates that both sites may function as hydrogen-bond donors toward bpca oxygen atoms.

Infrared Spectra of 1 and 2. The IR spectra of **1** and **2** have in common the presence of strong absorptions in the 3600−3400 cm^{-1} region (stretching OH vibrations of the water molecules) and a strong and sharp peak at 1710 cm^{-1} which is assigned to the ν(C═O) vibration of the carbonylimido group of the bpca ligand.[36,37] The most relevant feature of the IR spectrum of **1** is the shift toward higher frequency of the carbonyl stretching (strong and broad absorption at ca. 1730 cm^{-1}), which is centered at 1700 cm^{-1} in the IR spectrum of the potassium salts of 1,2-dtsq.[5] This feature, together with the occurrence of medium-intensity peaks at 1170 (ν(CCS)) and 900 cm^{-1} (ν(CS)) [1350, 1210 (ν(CCS)) and 930 cm^{-1} (ν(CS)) in the IR spectrum of the potassium salt],[5] is in agreement with the coordination of 1,2-dtsq to the metal through sulfur.[38] The IR bands of the 1,3-dtsq ligand in complex **2** are a sharp and strong peak at 1580 cm^{-1}, three medium-intensity absorptions at 1250, 1210, and 800 cm^{-1}, and a weak absorption at 825 cm^{-1}. These absorptions are to be compared with those centered at 1545 (ν(OCCCO)), 1260, 1210 (ν(CCS)), and 800 cm^{-1} (ν(CS)) in the IR spectrum of the free 1,3-dtsq anion.[17a] The higher frequency peak in the IR spectrum of **2** can be taken as indicative of bis-chelating 1,3-dtsq in copper(II) complexes.

Magnetic Properties of 1 and 2. The temperature dependence of $\chi_M T$ (χ_M being the magnetic susceptibility per four (**1**) and two (**2**) copper atoms) for complexes **1** and **2** is shown in Figures 5 and 6, respectively. The values of $\chi_M T$ at room temperature, 1.76 (**1**) and 0.86 $cm^3\ mol^{-1}\ K$ (**2**), are as expected for four (**1**) and two (**2**) noninteracting copper(II) ions. However, the shape of the $\chi_M T$ versus T curves is different. Upon cooling, the values $\chi_M T$ increase for complex **1**, attaining a maximum at 10 K, and then sharply decrease whereas, in the case of **2**, they decrease continuously and vanish at very low temperature. The susceptibility curve of **2** exhibits a maximum at 30 K (inset of Figure 6). These curves are characteristic of moderate ferro- (**1**) and antiferromagnetic (**2**) couplings.

Keeping in mind the tetranuclear structure of **1**, where two identical 1,2-dtsq-bridged copper(II) dimers are connected through weak axial Cu−S bonds with an inversion center being located at the center of the Cu(1)S(2)S(2a)Cu(1a) unit (Figure 2), the appropriate spin Hamiltonian (eq 2) with two exchange coupling constants J (coupling between Cu(1) and Cu(2)) and

(34) Procter, I. M.; Hathaway, B. J.; Nicholls, P. *J. Chem. Soc. A* **1968**, 1678.
(35) Castro, I.; Sletten, J.; Faus, J.; Julve, M.; Journaux, Y.; Lloret, F.; Alvarez, S. *Inorg. Chem.* **1992**, *31*, 1889.
(36) Castro, I.; Faus, J.; Julve, M.; Mollar, M.; Monge, A.; Gutiérrez-Puebla, E. *Inorg. Chim. Acta* **1989**, *161*, 97.
(37) Lerner, E. I.; Lippard, S. J. *Inorg. Chem.* **1977**, *16*, 1546.
(38) Sletten, J.; Julve, M.; Lloret, F.; Castro, I.; Seitz, G.; Mann, K. *Inorg. Chim. Acta* **1996**, *250*, 219.

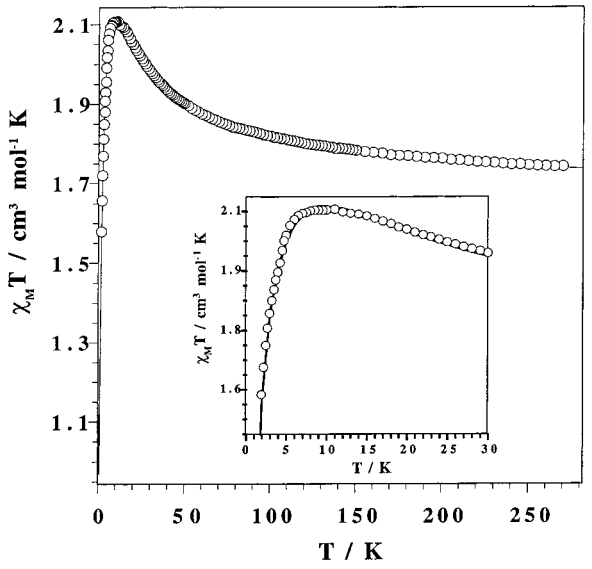

Figure 5. Thermal variation of $\chi_M T$ (χ_M being the magnetic susceptibility per four copper atoms) for **1**: (△) experimental data; (—) best fit (see text). The inset shows the maximum of $\chi_M T$ in the low-temperature region.

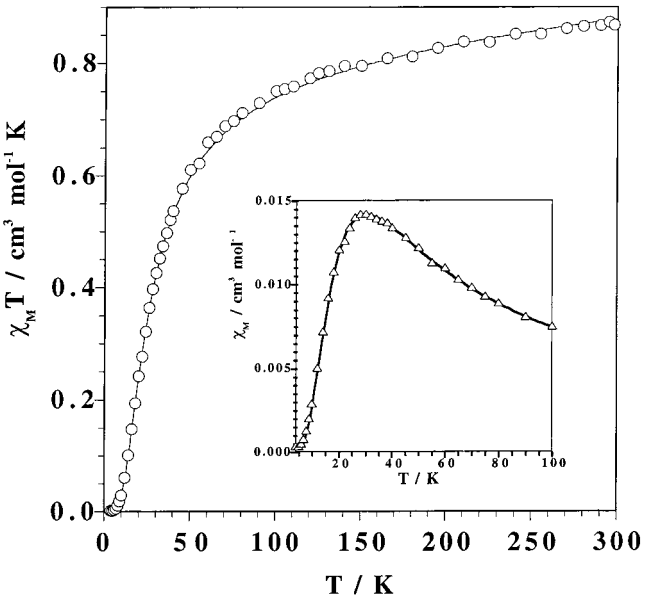

Figure 6. Thermal variation of χ_M and $\chi_M T$ (χ_M being the molar magnetic susceptibility) for **2**: (△) experimental data; (—) best fit (see text). The inset shows the maxium of χ_M in the low-temperature region.

J' (coupling between Cu(1) and Cu(1a)) was used to analyze its magnetic behavior. Least-squares fitting to the corresponding susceptibility expression (eqs 3−9) derived through this Hamiltonian by means of the Van Vleck formula and assuming identical Landé factors for the copper atoms, leads to $J = +32.4$ cm^{-1}, $J' = -5.0$ cm^{-1}, $g = 2.10$, and $R = 9.0 \times 10^{-5}$ (R is the agreement factor defined as $\sum_i[(\chi_M T)_{obs}(i) - (\chi_M T)_{calc}(i)]^2/\sum_i[(\chi_M T)_{obs}(i)]^2$). The theoretical curve matches very well the experimental data as indicated by the low value of the agreement factor. The fact that the magnetic interaction within the dinuclear unit is ferromagnetic may seem surprising at first sight. The weak antiferromagnetic coupling J' is easily understood on the basis of simple magnetic orbital considerations. In fact, the magnetic orbital on Cu(1) is of the $d_{x^2-y^2}$ type and is roughly defined by the N(1), N(2), N(3), and S(2) set of atoms. It is parallel with that centered on the symmetry-related Cu(1a) atom, which is separated from the former by 3.207(1) Å. In addition, these atoms are shifted in such a way that the equatorial S(2) atom at Cu(1) fills one of the axial sites at Cu(1a). Under these conditions, the overlap between both copper-centered magnetic orbitals is predicted to be very small, and consequently, a very weak magnetic coupling is expected, as observed. This weak antiferromagnetic interaction is responsible for the drop of the $\chi_M T$ curve below 10 K.

$$\hat{H} = -J(\hat{S}_1 \cdot \hat{S}_2 + \hat{S}_{1a} \cdot \hat{S}_{2a}) - J'(\hat{S}_1 \cdot \hat{S}_{1a}) \quad (2)$$

$$\chi_M T = (N\beta^2 g^2/k)[10\exp(-E_1/kT) + 2\exp(-E_2/kT) + 2\exp(-E_3/kT) + 2\exp(-E_4/kT)]/[5\exp(-E_1/kT) + 3\exp(-E_2/kT) + 3\exp(-E_3/kT) + 3\exp(-E_4/kT) + \exp(-E_5/kT) + \exp(-E_6/kT)] \quad (3)$$

$$E_1 = -J/2 - J'/4 \quad (4)$$

$$E_2 = J/2 - J'/4 \quad (5)$$

$$E_3 = J'/4 + (J^2 + J'^2)^{1/2}/2 \quad (6)$$

$$E_4 = J'/4 - (J^2 + J'^2)^{1/2}/2 \quad (7)$$

$$E_5 = J/2 + J'/4 + (4J^2 - 2JJ' + J'^2)^{1/2}/2 \quad (8)$$

$$E_6 = J/2 + J'/4 - (4J^2 - 2JJ' + J'^2)^{1/2}/2 \quad (9)$$

We have considered **2** as a 1,3-dtsq-bridged copper(II) dimer in a first approach. Consequently, its magnetic behavior was analyzed through a simple Bleaney−Bowers expression for two magnetically interacting local spin doublets derived through the Hamiltonian $H = -JS_1 \cdot S_2$ ($S_1 = S_2 = {}^1/_2$), where J is the magnetic coupling parameter. Least-squares fitting leads to $J = -33.5$ cm^{-1}, $g = 2.11$, and $R = 2.1 \times 10^{-5}$ (R is the agreement factor defined as $\sum_i[(\chi_M)_{obs}(i) - (\chi_M)_{calc}(i)]^2/\sum_i[(\chi_M)_{obs}(i)]^2$). Given that the 1,3-dtsq-bridged copper(II) dimeric units are linked through weak axial Cu−O(bpca) interactions (Figure 4), yielding an alternating copper(II) chain, the magnetic properties of this complex were also analyzed through the alternating-chain model by using the appropriate spin Hamiltonian (eq 10) where α is the alternating parameter and $S_{i-1} = S_i = S_{i+1} = {}^1/_2$.[39] The values of J, α, g, and R are −33.6 cm^{-1}, 0.065, 2.11, and 1.0×10^{-4}. The quality of the fit is close to that of the preceding one, the values of J and g are the same, and the value of αJ (−2.2 cm^{-1}) is very small. Both models are reasonable, but the former is the preferred one due to the smaller R value. Anyway, there is no doubt that the strongest antiferromagnetic coupling is mediated by the bis-chelating 1,3-dithiosquarate bridge, and in the context of the second model, the smallest magnetic interaction is to be ascribed to the out-of-plane CuO(1b)Cu(b)O(1) exchange pathway. In this compound, the two metal-centered magnetic orbitals are also of the $d_{x^2-y^2}$ type, being defined by the three bpca nitrogen atoms and the dithiosquarate sulfur atom. The low-spin density at the very weak axially coordinated bpca oxygen atom (2.903(8) Å for Cu−O(1b)) is at the origin of the poor overlap between the two parallel copper-centered magnetic orbitals, leading thus to a very weak exchange coupling if any.

$$\hat{H} = -J\sum_i(\hat{S}_{i-1} \cdot \hat{S}_i + \alpha\hat{S}_i \cdot \hat{S}_{i+1}) \quad (10)$$

Analysis of the Exchange Pathways through Bridging 1,*n*-Dithiosquarato Ligands in Complexes 1 and 2. The facts that

(39) (a) Duffy, W.; Barr, K. P. *Phys. Rev.* **1968**, *165*, 647. (b) Hall, J. W.; Marsh, W. E.; Welles, R. R.; Hatfield, W. E. *Inorg. Chem.* **1981**, *20*, 1033.

the magnetic couplings through 1,2-dtsq (**1**) and 1,3-dtsq (**2**) bridges are relatively strong (given the large metal−metal separation) and that they are of different natures are very interesting. To analyze the exchange pathways which are responsible for the ferro- (**1**) and antiferromagnetic (**2**) interactions observed, we have carried out DFT type calculations on the model systems shown in **I**−**III**, where the bpca nitrogen

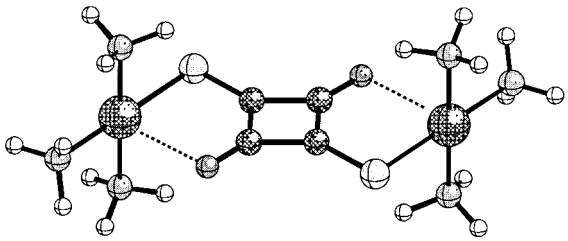

I

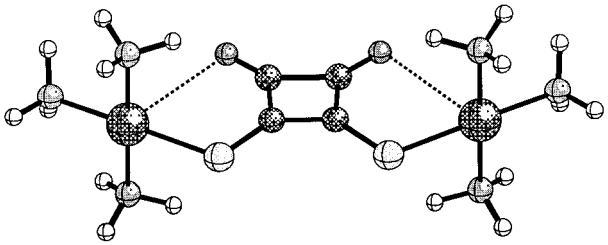

II

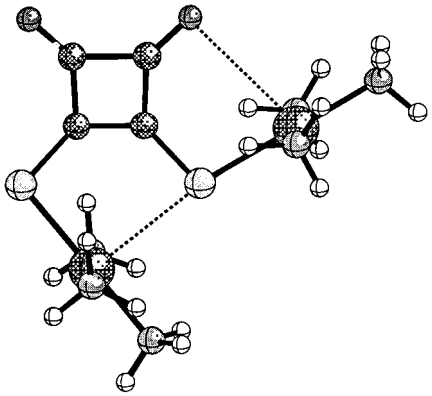

III

atoms have been replaced by three ammonia groups (the bond lengths and angles being those of the real structures).

The calculated values of J for models **I**−**III** are −43.3, −22.9, and −7.5 cm^{-1}, respectively. Focusing on the two first models, it is clear that the S−C−C−C−S skeleton of the 1,3-dtsq bridge is more efficient than the S−C−C−S skeleton of the 1,2-dtsq bridge in mediating antiferromagnetic interactions between the copper(II) ions. At first sight, this result seems quite surprising, given the greater length of the bridging skeleton in **I**. DFT calculations on the two bridging dithiosquarate ligands provide an orbital explanation for this apparent anomaly. The HOMO's of the 1,2- (ψ') and 1,3-dithiosquate ligands (ψ'') of appropriate symmetry to interact with the in-phase (ψ_u) and out-of-phase (ψ_g) combinations of the metal-centered magnetic orbitals as well as the resulting singly occupied molecular orbitals ψ_i with $i = 1-4$ (SOMO's) are shown in **4**. It can be seen, first, that the mean energy of the HOMO's of the 1,2-dtsq ligand is lower than that of the HOMO's of 1,3-dtsq and, second, that the energy gap of the corresponding SOMO's in the former (Δ') is smaller than that in the latter (Δ''). This trend is also reinforced by the larger energy gap between the HOMO's

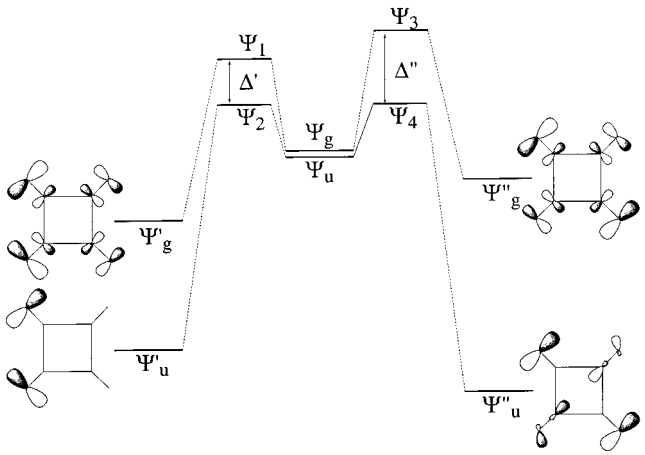

IV

of 1,3-dtsq as compared to that of 1,2-dtsq. According to the molecular orbital model by Hay et al.,[40] the value of J in a copper(II) dimer can be expressed by the sum of a ferromagnetic ($J_F > 0$) and an antiferromagnetic ($J_{AF} < 0$) contributions. Although two-electron integrals appear in this expression, it is generally accepted[41] that, within a family (Charts 1 and 2) of related compounds, the two-electron terms are nearly constant and the variations in the values of J are roughly related to the variations of the square of the energy gap between the SOMO's (Δ'^2 and Δ''^2 for 1,2- and 1,3-dtsq-bridged dimers). As $\Delta'^2 < \Delta''^2$, a larger antiferromagnetic coupling is expected for model **I** (compound **2**) as compared to model **II**. Given that the compound of model **II** has not been isolated, we cannot check this finding. Once the exchange pathway between two copper(II) ions through the S−C−C−C−S skeleton is established, it seems appropriate to compare its efficiency as an exchange mediator with that of the O−C−C−C−O skeleton in μ-1,3-squarato-bridged copper(II) dimers. In this regard, the value of J for the related complex $[Cu_2(bpca)_2(H_2O)_2(C_4O_4)]$ ($C_4O_4^{2-}$ is the dianion of 3,4-dihydroxycyclobuten-1,2-dione) is practically zero.[42] The smaller electronegativity and greater diffusiveness of sulfur compared to oxygen account for the greater efficiency of the S−C−C−C−S pathway. This is as observed when oxalato-bridged copper(II) complexes are compared with analogous compounds where the oxalato oxygen atoms are replaced by less electronegative atoms.[43,44]

When models **II** and **III** are compared, the bridging ligand being the same, the calculated value of J for **III** is significantly reduced relative to that of **II**. The molecular orbital analysis reveals that despite the different orientations of the two metal-centered magnetic orbitals, the overlap between them through the S−C−C−S skeleton is close to that of **II**. The occurrence of a new ferromagnetic exchange pathway in **III** (bond lengths and angles, the basal planes of the two copper atoms, and the position of sulfur therein are those of the real structure), that is Cu(1)−S(1)−Cu(2), has to be responsible for the lowering of the antiferromagnetic coupling in **III** as compared to that in **II**. The bridging sulfur S(1) in **1** occupies an equatorial position at Cu(2) but the axial one at Cu(1). So, the coupling between the

(40) Hay, P. J.; Thibeault, J. C.; Hoffmann, R. *J. Am. Chem. Soc.* **1975**, *97*, 4884.
(41) Alvarez, S.; Julve, M.; Verdaguer, M. *Inorg. Chem.* **1990**, *29*, 4500.
(42) Castro, I.; Faus, J.; Julve, M.; Journaux, Y.; Sletten, J. *J. Chem. Soc., Dalton Trans.* **1991**, 2533.
(43) Verdaguer, M.; Kahn, O.; Julve, M.; Gleizes, A. *Nouv. J. Chim.* **1985**, *9*, 325.
(44) Vicente, R.; Ribas, J.; Alvarez, S.; Seguí, A.; Solans, X. *Inorg. Chem.* **1987**, *26*, 4004.

two copper-centered magnetic orbitals through S(1) is expected to be ferromagnetic because the value of the Cu(1)−S(1)−Cu(2) angle (θ) is close to 180°. The value of this ferromagnetic interaction is predicted to decrease when θ decreases. According to the literature, a weak ferromagnetic coupling between copper(II) ions has been observed through a bridging sulfur atom in the copper(II) complex $[Cu(en)_2][Cu(1,2\text{-dtsq})_2]$.[13b] In this complex, the copper to bridging sulfur distances are 2.289(1) and 3.057(1) Å and θ is as small as 143.9(0)°. Given that the value of θ in **1** is somewhat larger (160.8°), the Cu(1)−S(1) and Cu(2)−S(1) bonds at the bridging sulfur being very close to the preceding ones, a significant ferromagnetic coupling through this pathway is ensured in **1**. Theoretical calculations for this exchange pathway according to the model shown in **5**

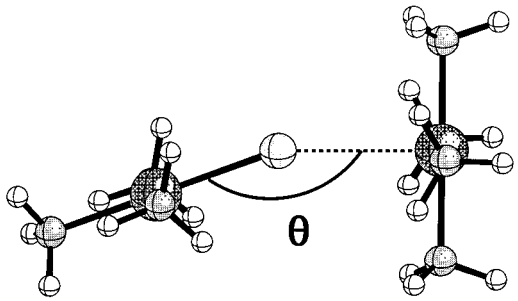

V

(θ being the variable parameter) reveal that the coupling is ferromagnetic (accidental orthogonality), it attains a maximum for θ equal to 180° (see Figure 7), and it becomes antiferromagnetic in the vicinity of $\theta = \sim 90°$.

The ferromagnetic coupling in **1** is thus due to the accidental orthogonality between the magnetic orbitals through the bridging S(1) atom. Its value is reduced by the antiferromagnetic coupling through the S−C−C−S pathway. The very high calculated J values are due to the simplicity of the model used, which was aimed at providing a qualitative explanation. The fact that each bpca group has been replaced by three ammonia ligands, the highly diffuse character of the sulfur orbitals, and the strong hybridization between the sp^3 ammonia and 3d metal orbitals favor the spin delocalization on the bridge and thus the magnitude of the exchange interaction.

Finally, once the exchange pathways in **1** and **2** are clearly established through simple models, we have calculated the J values for the real structures considering them as 1,2-dtsq- and 1,3-dtsq-bridged copper(II) dimers. The calculated values are +18 and −7 cm^{-1} for **1** and **2**, respectively, values which agree with the signs of the experimental ones and are quite close to them.They are also better than those calculated for the models **I** and **III** as expected, due to the effects that were introduced by the modelization and which have been discussed elsewhere.[45]

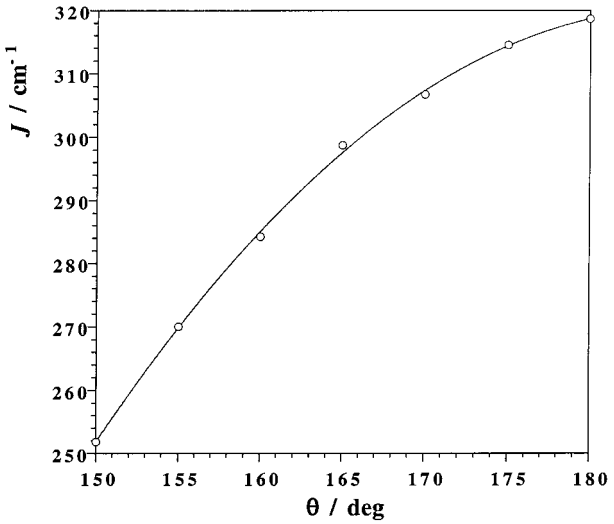

Figure 7. Plot of the calculated J value for model **V** as function of the angle at the bridging sulfur (θ).

Acknowledgment. Financial support from the Spanish Dirección General de Investigación Científica y Técnica (DGICYT) (Project PB97-1397) is gratefully acknowledged. Computer resource support for this work was provided by the Centre d'Informàtica de la Universitat de València. We are indebted to Dr. J. A. Moreno from the University of Granada for growing crystals of complex **2** by the gel technique.

Supporting Information Available: X-ray crystallographic files, in CIF format, and tables of crystal data and X-ray experimental details, anisotropic displacement parameters for non-hydrogen atoms, atomic fractional coordinates and U(eq) values, complete bond lengths and angles, least-squares planes, and hydrogen bond distances for **1** and **2**. This material is available free of charge via the Internet at http://pubs.acs.org.

IC9904384

(45) Ruiz, E.; Alemany, P.; Alvarez, S.; Cano, J. *Inorg. Chem.* **1997**, *36*, 3683.